Geophysical Research Letters

RESEARCH LETTER
10.1029/2021GL095955

# Orbital Forcing Strongly Influences the Poleward Shift of the Spring Himalayan Jet During the Past Millennium

U. K. Thapa[1,2], S. Stevenson[1], and M. Midhun[1,3]

[1]Bren School of Environmental Science and Management, University of California Santa Barbra, Santa Barbara, CA, USA, [2]University Corporation for Atmospheric Research, Boulder, CO, USA, [3]Department of Atmospheric Sciences, Cochin University of Science and Technology, Kochi, India

**Key Points:**

- Climate model simulations indicate an orbitally forced trend in the position of the Himalayan subtropical jet over the past millennium
- The orbitally forced decline in thermal gradient between the equator and subtropical Asia shifted the spring jet poleward during 850–1849
- During the twentieth century, the orbital-forced poleward trend in the spring Himalayan jet position is masked by greenhouse gas forcing

**Supporting Information:**

Supporting Information may be found in the online version of this article.

**Correspondence to:**

U. K. Thapa,
udaythapa@ucar.edu

**Citation:**

Thapa, U. K., Stevenson, S., & Midhun, M. (2022). Orbital forcing strongly influences the poleward shift of the spring Himalayan jet during the past millennium. *Geophysical Research Letters*, *49*, e2021GL095955. https://doi.org/10.1029/2021GL095955

Received 11 SEP 2021
Accepted 11 JAN 2022



**Abstract** The latitudinal position of the subtropical jet over the Himalayas (Himalayan jet latitude or HJL) controls the region's climate during winter and spring by guiding moisture-delivering storms. Here we use the Community Earth System Model-Last Millennium Ensemble to diagnose forced trends in HJL during the past millennium. During 850–1849, there is a weak equatorward trend in winter HJL. In contrast, the spring HJL has a relatively larger poleward trend, and increases in both variance and frequency of poleward/equatorward excursions. We demonstrate changes in orbital precession reduced the thermal gradient between tropical and subtropical Asia, shifting the spring HJL poleward. During 1850–2005, the spring HJL exhibits no trend due to compensating influences from orbital and anthropogenic greenhouse gas forcings. These findings suggest it is essential climate models properly simulate the effects of and potential interactions between orbital forcing and anthropogenic factors to accurately project Himalayan jet variability and associated storm tracks.

**Plain Language Summary** The subtropical jet stream (STJ) guides storms into the Himalayan region, which deliver snow and rainfall that are the region's primary source of water during winter and spring. However, little is known about the impacts of long-term climatic changes on the behavior of the STJ over the Himalayas (Himalayan jet). In this study, which is first of its kind, we use the Community Earth System Model-Last Millennium Ensemble to investigate the impacts of natural and anthropogenic factors on the location of the Himalayan jet during the past millennium. During the pre-industrial period (850–1849), we show that, compared to the weak equatorward trend in winter, the spring Himalayan jet shifted poleward and displayed increased variability. These effects arise from orbitally driven reductions in the temperature difference between the tropics and the subtropical Asia. The pre-industrial poleward trend in the orbital-only spring Himalayan jet latitude also exists post 1850, but that trend is canceled by the twentieth century greenhouse gas forcing. Our results suggest it is critical to ensure climate models properly simulate responses to both orbital forcing and anthropogenic factors in order to accurately project future Himalayan jet variability and associated storm tracks in the face of global warming.

## 1. Introduction

The subtropical jet stream (STJ), which passes immediately south of the Himalayas (27–30°N) during boreal winter and spring (Koteswaram, 1953; Koteswaram et al., 1953), controls the climate of the region by guiding storms into the Himalayas (Dimri et al., 2015). These storms, commonly known as western disturbances, deliver snow in the mountains and rainfall at lower altitudes (Cannon et al., 2015, 2016; K. M. R. Hunt et al., 2018; Madhura et al., 2015), providing water to more than 1 billion Asian people for agriculture and power generation during the dry seasons (Biemans et al., 2019; Immerzeel et al., 2020; Nie et al., 2021). The STJ also regulates the meridional movement of tropical air masses. When the STJ moves poleward, the Himalayan region receives reduced number of storms, and warm tropical air is able to advect into higher latitudes, making the region both hotter and drier (Ahmed et al., 2020; K. M. R. Hunt et al., 2018; Thapa et al., 2020; Wang et al., 2013; Yin, 2005; Zhang et al., 2006). It is possible warm tropical air could bring moisture with it, but the Himalayas remain drier than normal due to decreased number of western disturbances and increased evaporative demand during the poleward displacement of the jet (Ahmed et al., 2020; K. M. R. Hunt et al., 2018; Schiemann et al., 2009; Thapa et al., 2020). In contrast, equatorward jet displacement steers more storms into the Himalayas, making the region wetter than normal (Schiemann et al., 2009). Therefore, changes in the position of the STJ have implications for regional water supply and management.

Observational studies show no significant trend in mean jet latitude over Asia during recent decades (Kuang & Zhang, 2005; Thapa et al., 2020; Zhongda & Riyu, 2005), in contrast to the poleward trend in hemispheric-mean circulation (Archer & Caldeira, 2008; Fu et al., 2006; Maher et al., 2020; Manney & Hegglin, 2018; Pena-Ortiz et al., 2013; Strong & Davis, 2007). Similarly, reconstructions do not show any trends in the STJ latitude over central and eastern Asia during the past millennium (Thapa et al., 2020; Wright et al., 2015). Model simulations of summer jet over eastern and western Asia also show no long-term trend in its location (Jiang et al., 2020). However, there has been a significant increase in interannual STJ variance over central and East Asia during the past millennium (Jiang et al., 2020; Thapa et al., 2020; Wright et al., 2015). In addition, a recent tree-ring reconstruction shows a positive trend in extreme poleward excursions of the spring STJ over the Himalayas during the past four centuries (Thapa et al., 2020). Understanding the dynamics of potential forced trends in the mean and extreme positions of the jet is needed to determine its sensitivity in the face of anthropogenic climate change.

Because of the large extent of internal climate variability, understanding the mechanisms for long-term jet variations requires an ensemble approach in order to provide robust statistics. For this purpose, the Community Earth System Model-Last Millennium Ensemble (CESM-LME) simulations are an ideal tool, being one of the only available ensembles covering the full 850–2005 CE period (Otto-Bliesner et al., 2016). The CESM-LME ensembles comprise: "single-forcing" simulations including individual external forcing factors, namely land use and land cover change (LULC), ozone/aerosols, greenhouse gases, solar irradiance, orbital forcing, and volcanic eruptions; and "fully forced" simulations that include all forcing factors, simultaneously (Otto-Bliesner et al., 2016). The CESM-LME has been used to study many aspects of climate and are able to capture the observed character of climate variability (Capotondi et al., 2020; Marcello et al., 2019; Stevenson, Fasullo, et al., 2017; Stevenson, et al., 2018). The CESM-LME therefore provides an excellent opportunity to diagnose forced trends in STJ position over the Himalayas during the past millennium.

## 2. Data and Methods

### 2.1. Model Simulations and Reanalysis Products

We used all single and full-forcing members of CESM-LME version 1 (CESM1), which extend from 850 to 2005 CE (Otto-Bliesner et al., 2016; Table S1 in Supporting Information S1). The CESM1 was run using an atmospheric and land resolution of 2°, and an ocean and sea ice resolution of 1°. We note that the ozone/aerosol forcing data set only extends over 1850–2005 (Otto-Bliesner et al., 2016) due to a lack of anthropogenic ozone/aerosol forcing information prior to 1850.

In order to evaluate model performance in reproducing STJ properties, we used monthly wind data from several reanalyzes including the National Centers for Environmental Prediction-National Center for Atmospheric Research (NCEP/NCAR) 40-year reanalysis project (Kalnay et al., 1996), the ERA-5 (Bell et al., 2020; Hersbach et al., 2018), the Japanese 55-year Reanalysis (Kobayashi et al., 2015), and the twentieth Century Reanalysis-Version3 (Slivinski et al., 2019). Based on its comparatively reliable jet variance and longer calibration period, we chose to use NCEP/NCAR data, which has a 2.5°resolution, as the primary validation data set (see Thapa et al., 2020 for a detailed explanation).

### 2.2. Himalayan Jet Latitude (HJL) Calculation and Variability

We calculated an index for the latitudinal position of the STJ over the Himalayan longitudes: 70–95°E. The position of the STJ for each longitude grid was identified as the latitude corresponding to the maximum average seasonal wind speed at 200mb (Barton & Ellis, 2009; Belmecheri et al., 2017; Koch et al., 2006; Trouet et al., 2018). We defined this index as the Himalayan jet latitude (HJL), and computed that index for each forcing for both winter and spring seasons using CESM1 monthly scalar wind data. We identified the cases of extreme northerly or southerly displacements by the Himalayan jet as "poleward" or "equatorward excursions" when the latitude exceeded two or more standard deviations from the mean position.

To examine the interannual variability in the HJL over time, we calculated the coefficient of variance (standard deviation/mean) as well as jet excursions over a 31-year time window. Linear regression coefficients were used to identify the presence of significant trends in HJL, running variance, and excursions over the last millennium. We

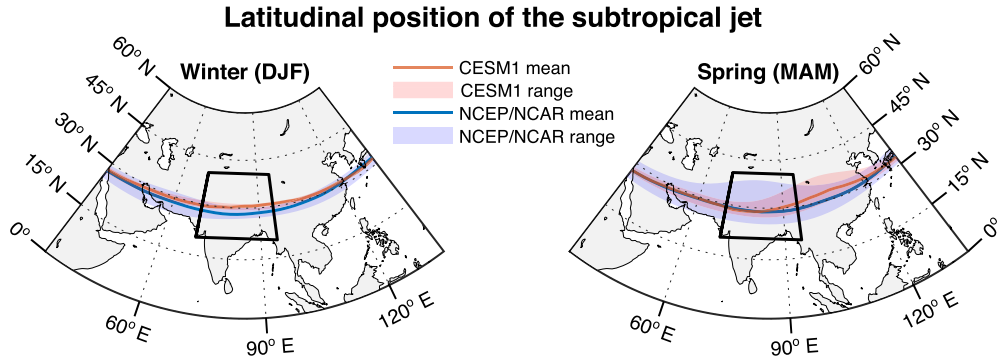


**Figure 1.** Comparison of the subtropical jet latitude based on fully forced CESM-LME version 1 simulations (orange) with the National Centers for Environmental Prediction-National Center for Atmospheric Research Reanalysis-based jet latitude (blue) for the period of 1948–2005. Solid lines represent the mean latitudinal positions of the subtropical jet stream whereas the shades represent its maximum and minimum latitudes (i.e., range). Inset represents the geographical focus of the current study, the Himalayan region; 70–95°E and 20–40°N.

employed linear regressions on 20-year Gaussian smoothed versions of HJL time series. Forced trends in HJL are considered separately for the two periods: 850–1849 CE (pre-industrial) and 1850–2005 CE (twentieth century).

## 3. Results and Discussion

### 3.1. Model Performance

The CESM1 underestimates the range of STJ latitudes in reanalysis data but does a fair job in capturing the observed mean position and strength of the STJ over 1948–2005 (Figures 1 and S1 in Supporting Information S1). The CESM1 also reproduces the observed jet position over the larger geographical domain spanning from the Middle East to the western Pacific, but simulates a higher jet latitude over the Himalayas and Tibetan Plateau by about 2.5° in some grids in both winter and spring (Figure 1). The CESM1 also overestimates the magnitude of interannual variability in HJL in all reanalysis products (Figure S2 in Supporting Information S1), with the exception of the early portions of the ERA5 and 20th century reanalysis products, which are likely unreliable.

### 3.2. Trends in Mean HJL

There is a small but statistically significant negative trend ($-0.26 \times 10^{-2\circ}$ century$^{-1}$, $p < 0.01$) in the mean position of the pre-industrial fully forced winter HJL (Figures 2a, 3a and S3 in Supporting Information S1). This trend differs from the recently observed poleward trend in global STJs and tropical belt in both hemispheres (Manney & Hegglin, 2018; Pena-Ortiz et al., 2013; Staten et al., 2018). There is a relatively larger poleward shift ($3.18 \times 10^{-2\circ}$ century$^{-1}$, $p < 0.01$) in the pre-industrial fully forced spring HJL (Figures 2a, 3a and S3 in Supporting Information S1).

Over the pre-industrial period, volcanic eruptions contributed to the equatorward trend in winter HJL, while LULC and natural factors including solar irradiation and orbital forcing reduced the magnitude of that trend (Figure 3a). Similar to the fully forced HJL, there are strong and significant positive trends in solar-, and specifically orbital-only ($p < 0.01$) forced spring HJL, indicating that these natural factors helped shift the pre-industrial spring jet toward the pole (Figure 3a).

During the twentieth century, there is a small equatorward trend ($-0.5 \times 10^{-3\circ}$ year$^{-1}$, $p < 0.01$) in the fully forced winter HJL but no significant trend in spring HJL (Figure 3). The lack of trend in spring HJL is consistent with observations that do not show any significant trend in the mean position of STJ over Central and East Asia (Kuang & Zhang, 2005; Thapa et al., 2020; Zhongda & Riyu, 2005), but CESM1-based trends differ from the general poleward shift of STJs in both hemispheres in recent decades (Archer & Caldeira, 2008; Fu et al., 2006; Maher et al., 2020; Manney & Hegglin, 2018; Pena-Ortiz et al., 2013; Strong & Davis, 2007).

The anthropogenic factors tend to cancel each other's effects on the twentieth century trends in jet latitude (Figure 3b). In the case of winter, the greenhouse gas forcing shifted the jet poleward which is canceled by the

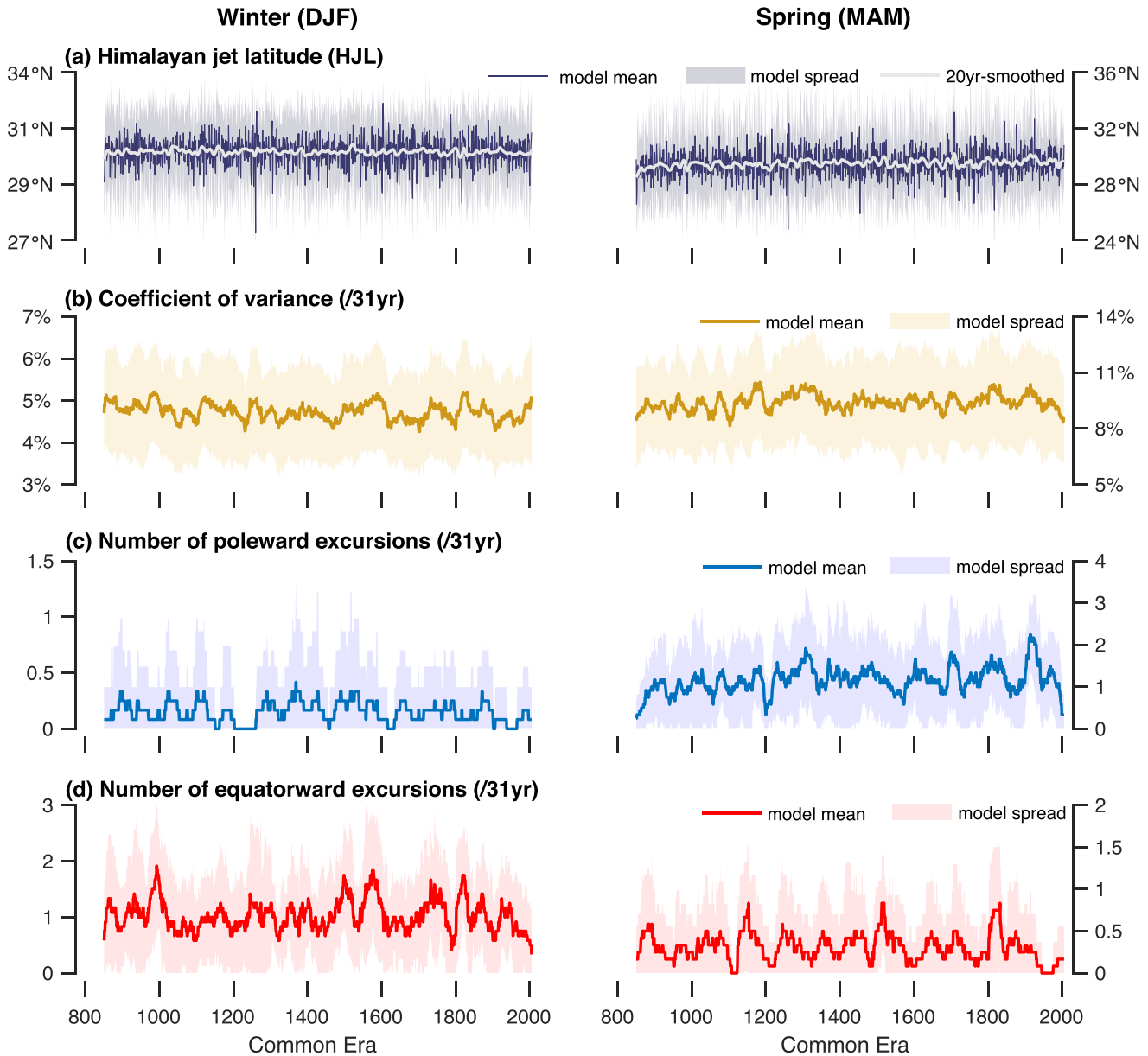


**Figure 2.** Variability in the (left) winter and (right) spring Himalayan jet latitude (HJL) in the CESM-LME version 1 full-forcing ensemble simulations during 850-2005. (a) Time series of the mean HJL, and (b) the coefficient of variance in HJL, (c) the frequency of poleward excursions and (d) equatorward excursions by the Himalayan jet over the 31-year window. The model spread (standard deviation across the ensemble members) is shown by color shading and the ensemble mean of 12 fully forced members is shown in solid line.

negative trend in LULC, resulting in a small equatorward trend in fully forced simulations. During spring, the greenhouse gas forcing displaced the Himalayan jet toward the equator and the ozone and aerosol forcing toward the pole, canceling each other and therefore resulting in no significant trend in HJL. Similar cancellations between greenhouse gas and aerosol forcing have also been found in several other aspects of climate variability (Stevenson, Capotondi, et al., 2017; Touma et al., 2021). The equatorward trend in spring Himalayan jet in greenhouse gas-only forcing is consistent with the projected equatorward shift of the STJ under global warming (Zhou et al., 2019).

The positive trend in spring HJL seen in CESM-LME simulations appears to differ from existing proxy reconstructions. For instance, the tree-ring reconstruction of spring HJL presented in Thapa et al., 2020 exhibited a relatively small and statistically insignificant poleward trend over the past four centuries ($2 \times 10^{-2}$° century$^{-1}$,

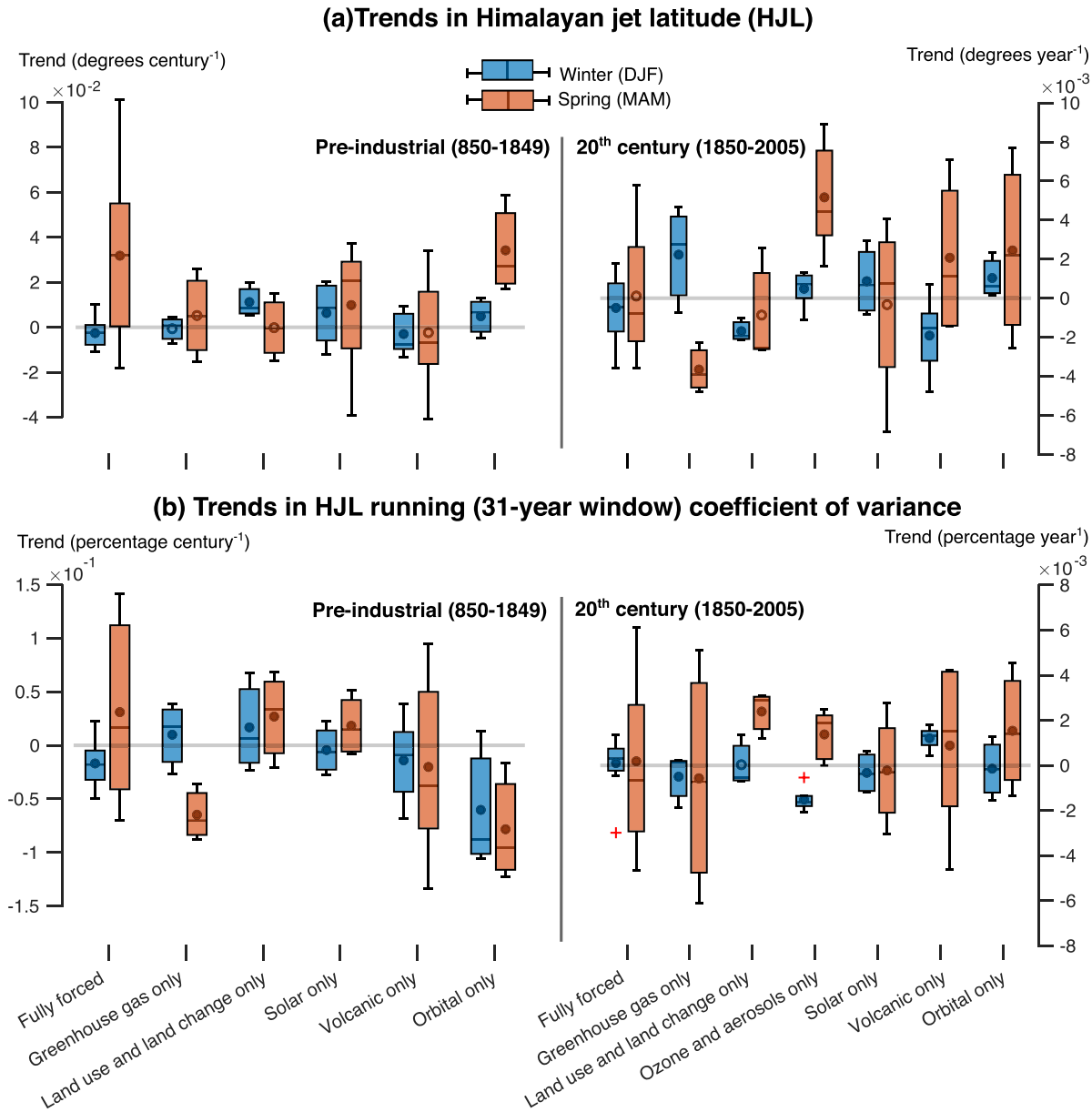


**Figure 3.** Boxplots showing distribution of trends in (a) the mean Himalayan jet latitude (HJL) and (b) running HJL coefficient of variance over a 31-year window across all individual ensemble members for all CESM1 forcings during 850–1849 and 1850–2005. Blue and orange boxes represent distribution of trends for winter (DJF) and spring season (MAM), respectively. Circle (open or closed) in each box represents the mean trends across all ensemble members for respective forcing. The closed circles are mean trends that are significant at the 0.01 level.

$p = 0.22$; Figure S4a in Supporting Information S1). Similarly, the reconstructed position of the jet stream over East Asia also does not display any multicentury trend (Wright et al., 2015).

### 3.3. Trends in HJL Variance

There is a significant decline ($-0.17 \times 10^{-1}$ percentage century$^{-1}$, $p < 0.01$) in the fully forced winter HJL variance and a significant increase ($0.31 \times 10^{-1}$ percentage century$^{-1}$, $p < 0.01$) in spring HJL variance over the pre-industrial period (Figures 2b, 3b and S5 in Supporting Information S1). The single-forcing LME simulations indicate that natural factors (solar, volcanic and orbital forcings) caused a decline in the pre-industrial winter HJL variance, while the anthropogenic influences (greenhouse gas and LULC forcings) counteracted these effects (Figure 3b). During spring, the split between natural and anthropogenic influences is less clear: LULC- and

solar-only forcings have positive trends similar to fully forced simulations, suggesting their roles in the simulated increase in spring jet variance. In contrast, most of the other pre-industrial single-forcing simulations (greenhouse gases, volcanic and orbital) acted to decrease HJL variance. We acknowledge the combination of pre-industrial single-forcing variances does not reproduce the fully forced jet variance that suggests considerable possible non-linear interactions amongst the forcings.

During the twentieth century, both the winter and spring Himalayan jet exhibited small increases ($p < 0.01$) in variance with positive contributions from volcanic and orbital forcings (Figure 3b). The greenhouse gas forcing tends to cancel the effects of natural forcings, reducing variance during both seasons. Tree-ring reconstructions show enhanced variance in jet position over Asia during the twentieth century (Thapa et al., 2020; Wright et al., 2015). In other regions, observation- and model-based studies also demonstrate enhanced variability since the mid-twentieth century, and this trend has been attributed to anthropogenic climate change (Barnes & Polvani, 2013; Coumou et al., 2015; Francis & Vavrus, 2012; Mann et al., 2017). It is possible the structure or strength of the jet could contribute to the enhanced variance in observations or reconstructions, but studies have demonstrated greater role of jet position in regulating regional climate compared to other jet metrics (K. M. R. Hunt et al., 2018; Schiemann et al., 2009; Thapa et al., 2020), because of which we focused on its latitude based on strongest wind in the current study.

When compared over the period of overlap (1625–2003), the HJL variance in CESM1 does not match with tree-ring reconstruction. The CESM1 shows a negative trend in spring HJL over the past four centuries, which is different from the positive trend in tree-ring reconstructed variance in spring jet latitude (Thapa et al., 2020; Figure S4b in Supporting Information S1). The CESM1 also overestimates the magnitude of variance relative to the reconstruction.

### 3.4. Trends in Himalayan Jet Excursions

Over the pre-industrial period, the fully forced CESM1 simulations show no significant change in the frequency of winter poleward jet excursions (Figures 2c, S6a and S7a in Supporting Information S1), while equatorward excursions have increased significantly ($0.11 \times 10^{-1}$ counts century$^{-1}$, $p < 0.01$; Figures 2d, S7b and S8a in Supporting Information S1). During spring, both poleward and equatorward excursions increase significantly (Figures 2c and 2d and S6–S8 in Supporting Information S1), but the poleward trend has a larger magnitude. This is consistent with tree-ring evidence for an increase in spring poleward jet excursions, although the simulated increase in equatorward excursions is not present in tree-ring reconstruction (Thapa et al., 2020).

The lack of change in winter poleward excursions appears to result from a cancellation between greenhouse and solar forcings (Figure S7a in Supporting Information S1). In contrast, the trend in winter equatorward excursions appears to result from greenhouse forcing (Figure S7b in Supporting Information S1), a striking result given that the pre-industrial GHG emissions changes are quite small. These GHG-driven trends are compensated by significant negative trends caused by volcanic and orbital forcings (Figure S7b in Supporting Information S1).

Poleward excursions during spring increase in the orbital-, solar- and LULC-only simulations. The orbital forcing signal is particularly strong, suggesting a dominant role for orbital changes (Figure S7a in Supporting Information S1). In contrast, spring equatorward extremes decrease due to solar-, orbital- and greenhouse (Figure S7b in Supporting Information S1). Interestingly, the LULC-only forcing has a significant positive trend ($p < 0.01$), suggesting a role of changes in land use practices in increasing the cases of equatorward excursions by the spring Himalayan jet.

During the twentieth century, both winter and spring Himalayan jets showed decreased trends in the frequency of both poleward and equatorward excursions (Figure S9a and S9b in Supporting Information S1). However, the small numbers of twentieth century events (often close to zero) make it difficult to draw robust conclusions regarding forced trends over this shorter time period.

### 3.5. Dynamics of Forced Trend in Spring HJL

We examined possible mechanisms for forced trends in the HJL by mapping the trends in surface temperature (TS), sea-level pressure (SLP), and 200mb temperature (T200), geopotential heights (height) and 200mb zonal winds (U). In the full-forcing simulations, positive trends occur over the pre-industrial period in spring TS

(Figure 4a), T200 (Figure S10 in Supporting Information S1) and height (Figure S11 in Supporting Information S1) in subtropical/central Asia, while negative SLP trends exist over most of subtropical Asia (Figure S12 in Supporting Information S1). Additionally, significant trends occur in 200mb spring winds over central Asia: trends are positive in the northern latitudes and negative in the southern latitudes (Figure 4b). This is consistent with previous works indicating the ability of subtropical warming to shift the subtropical jet poleward by decreasing the temperature gradient between the equator and the subtropics (Fu et al., 2006; Fu & Lin, 2011; Hu & Fu, 2007; Rotstayn et al., 2013; Seidel et al., 2008; Wilcox et al., 2012).

When the patterns of trends in the single-forcing ensembles are examined, orbital forcing emerges as the most likely cause of the jet shifts (Figure 4a and 4b). The orbital-only ensemble has trends similar to the full-forcing simulations in all variables over the Asian region: significant positive trends in 200mb winds at northern latitudes and negative trends at southern latitudes of central Asia, warming over subtropical Asia, and increased 200mb geopotential heights as well as T200 over the Indian subcontinent.

Because changes in earth's orbital parameters affect insolation by latitude and season, which can alter large-scale climate and circulation systems (Borisenkov et al., 1983; Davis & Brewer, 2009; Laskar et al., 1993; Lücke et al., 2021), we looked at insolation received at 30°N latitude and equator (0°) using values of eccentricity, obliquity and precession from Berger and Loutre (1991). We found that, during the past millennium, the latitudinal difference in insolation between 30°N and the equator increased during spring (0.004 $Wm^{-2}$ $decade^{-1}$, $p < 0.001$) and decreased slightly for winter (−0.002 $Wm^{-2}$ $decade^{-1}$, $p < 0.001$; Figure 5a). This is accompanied by a significant decline in temperature difference between the tropics (5°S–5°N) and the subtropics (25–35°N) in spring for the fully forced ($-1.4 \times 10^{-2}$°C $century^{-1}$, $p < 0.001$) and orbital-only ($-2.5 \times 10^{-2}$°C $century^{-1}$, $p < 0.001$) simulations (Figure 5b). This finding suggests that orbital forcing has a strong influence on the poleward shift of spring HJL during the past millennium, consistent with other recent work demonstrating the ability of orbital forcing to affect millennial trends in proxy reconstructions (Lücke et al., 2021).

This effect seems much smaller in winter: although there is a slight equatorward HJL trend which might indicate an influence from the reduced insolation gradient (Figure 5a), the tropical-subtropical thermal gradient does not exhibit a significant trend (Figure S14 in Supporting Information S1).

The orbitally driven poleward trend in spring HJL continues throughout the twentieth century, but post 1850, that trend is masked by the greenhouse gas forcing (Figure 3a). When mapped over the twentieth century (Figure S15 in Supporting Information S1), there is uniform cooling over most parts of Asia in the ozone and aerosol-only forcing simulations, which could be due to the cooling effects of aerosols over the Indian subcontinent (Krishnan & Ramanathan, 2002). This aerosol-driven increase in the thermal gradient likely cancels the effects of greenhouse gas forcing. The lack of apparent twentieth century subtropical warming over Asia might explain the lack of trend in the mean position of spring jet or equatorward trend in the fully forced winter jet during this period (Figure S16 in Supporting Information S1). This outcome is also supported by the lack of significant trend in tropical-subtropical thermal gradient in spring and a significant positive trend ($p < 0.01$) in winter in the fully forced simulations (Figure S17 in Supporting Information S1).

## 4. Conclusions

The HJL is the primary control on the region's hydroclimate during winter and spring, affecting water supply for nearly 1 billion Asian people. In this study, which is the first of its kind in the region, we used the CESM-LME to diagnose forced trends in the HJL and its variance spanning the past millennium. Compared to the weak negative trend in winter HJL, the spring HJL has stronger and significant poleward trend over the pre-industrial period. The spring HJL also exhibited significant positive trends in interannual variability as well as in the frequency of poleward and equatorward excursions. During the twentieth century, the weak equatorward trend in winter HJL continues, while the spring HJL does not exhibit any significant trend. As suggested by earlier studies (Grise et al., 2018; Maher et al., 2020), our results also confirm that the jet properties can vary by season and region even when a longer time period is considered.

Our results suggest that orbital forcing has a strong influence on the poleward shift of the spring Himalayan jet, and in fact constitutes the dominant pre-industrial forcing. Changes in earth's axial precession increased the difference in spring insolation received between the subtropics and equator over the course of the last millennium.

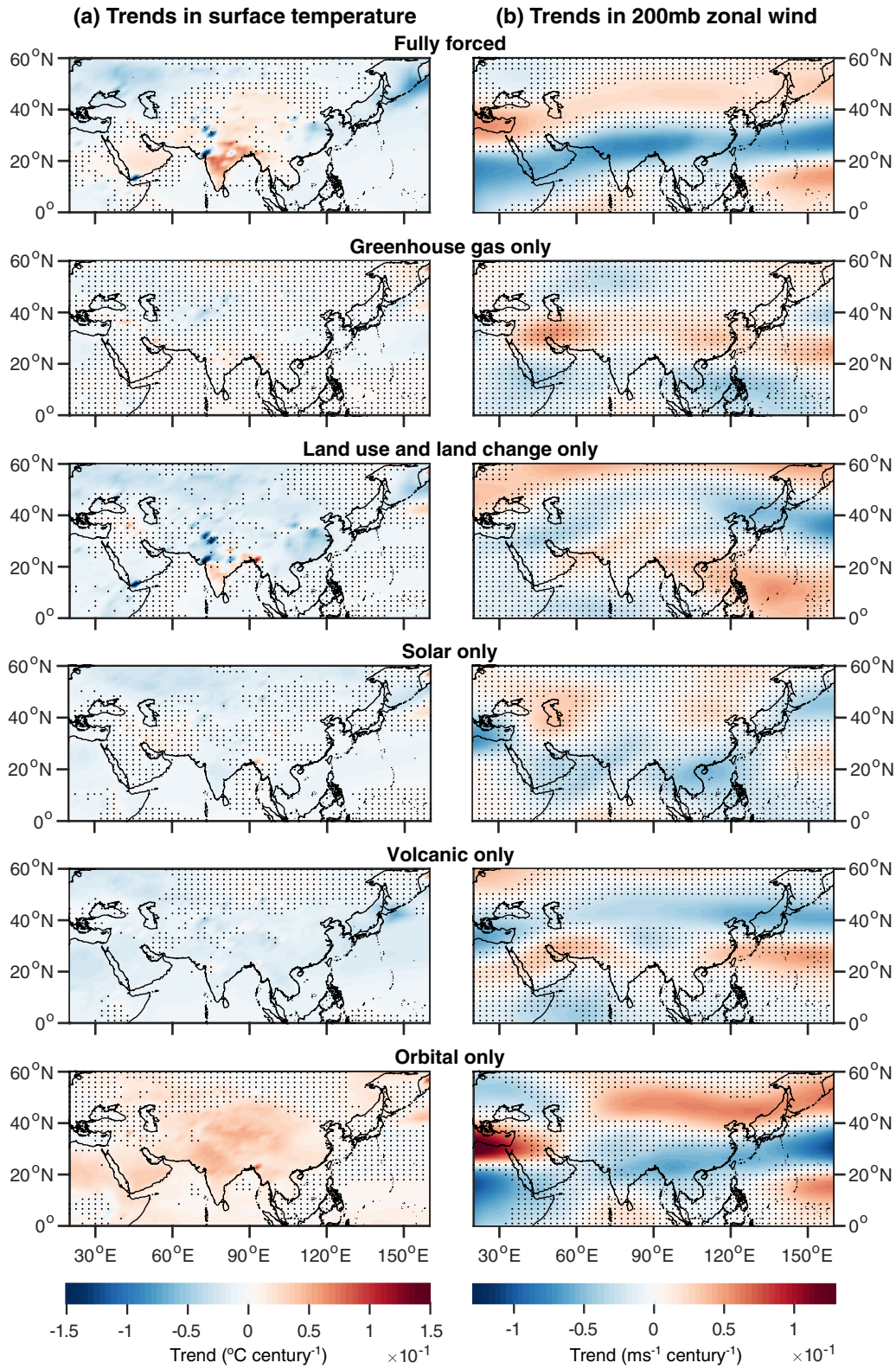


**Figure 4.** Mean trends in spring (a) surface temperature and (b) 200mb zonal winds during 850–1849 across all CESM-LME version 1 ensembles for all forcings. Stippling indicates the trends that are not significant at the 0.01 level. Interestingly, this similarity is only apparent in the spring; the forced trends in Winter-Time variables do not resemble one another in the fully forced and orbital-only ensembles (Figures S10–S13 in Supporting Information S1).

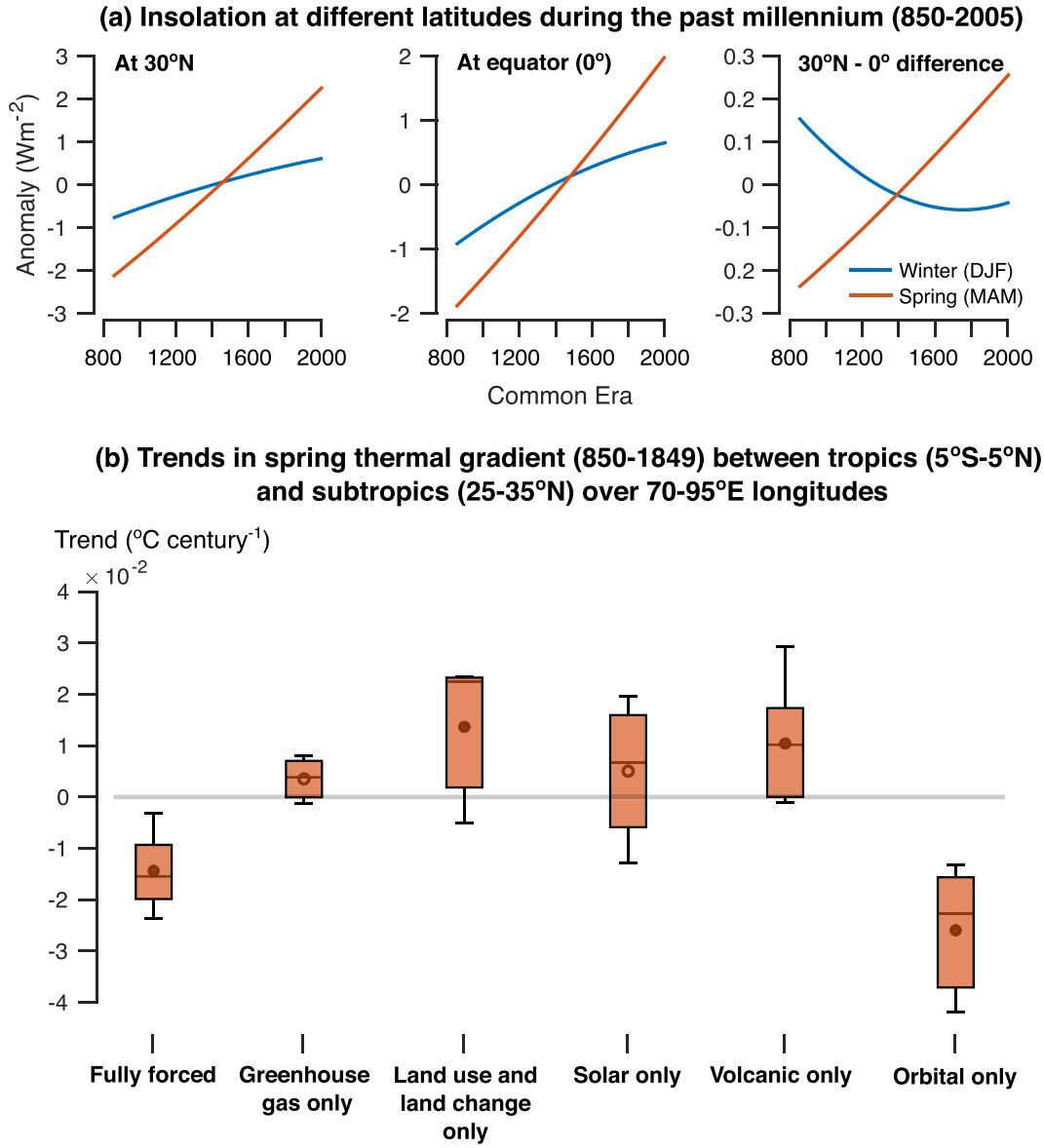


**Figure 5.** Daily insolation at different latitudes and thermal gradient between tropics and subtropical Asia. (a) Daily insolation received at 30°N, equator (0°) and difference between the two during 850–2005. (b) Boxplots showing distribution of trends in the spring temperature difference between tropics (5°S–5°N) and subtropics (25–35°N) over 70–95°E longitudes across all individual ensemble members for all CESM1 forcings during 850–1849. Circle (open or closed) in each box represents the mean trends across all ensemble members for respective forcing. The closed circles are mean trends that are significant at the 0.01 level.

This difference in insolation caused the subtropics to warm faster than the tropics, reducing the thermal gradient between the tropics and subtropical Asia, which in turn facilitated the poleward shift of the spring HJL. The pre-industrial poleward trend in orbital-only spring HJL also exists post 1850, but that trend is canceled by the twentieth century greenhouse gas forcing. In the context of the past millennium, orbital forcing is known to have weaker effects on climate compared to volcanism and other natural influences (Crowley, 2000; Servonnat et al., 2010). However, based on our results, we argue that the impact of orbital forcing on Himalayan jet variability cannot be overlooked even when only the past millennium is considered.

Both CESM1 and a previously published tree-ring reconstruction (Thapa et al., 2020) show a small poleward trend in spring HJL over the past four centuries, but they differ in the trend and magnitude of variance. This proxy-model discrepancy might be because of the shorter reconstruction period or an underestimation of observed variance

by the proxy. Next, because there is no sharp boundary between the STJ and polar jet over Asia (Ren et al., 2011), it is possible temperature changes over high-latitude Asia could also affect the HJL, but CESM1 underestimates warming over northern Asia and southern China (Figures S18 and S19 in Supporting Information S1), which could also possibly result in proxy-model mismatch. We note that data limitations necessitated the use of a single model in this study, and that CESM1 is biased toward overestimating both observed mean HJL and its variance during both winter and spring seasons (Figure S2 in Supporting Information S1), which might have affected our results. Nevertheless, based on our findings, it is clear that orbital forcing strongly influences spring jet variability over the past millennium. Our results imply that correctly capturing low-frequency (centennial-millennial) variability in jet behavior may require ensuring that climate models properly simulate both the response to orbital forcing and potential nonlinear interactions between orbital forcing and anthropogenic impacts.

## Data Availability Statement

All data used in this study are publicly accessible. The CESM-LME simulations are available at Climate Data Gateway at NCAR (https://www.earthsystemgrid.org/dataset/ucar.cgd.ccsm4.cesmLME.html). The NCEP/NCAR Reanalysis (https://psl.noaa.gov/data/gridded/data.ncep.reanalysis.html), the twentieth Century Reanalysis (https://psl.noaa.gov/data/gridded/data.20thC_ReanV3.html) and the observed sea-surface temperatures (https://psl.noaa.gov/data/gridded/data.noaa.ersst.v5.html) were obtained from the NOAA Physical Sciences Laboratory website. The JRA-55 and ERA-5 Reanalysis wind data were accessed from the NCAR Climate Data Guide (https://rda.ucar.edu/datasets/ds628.1/) and https://confluence.ecmwf.int/display/CKB/The+family+of+ERA5+datasets, respectively. The tree-ring reconstructions were downloaded from the NOAA World Data Center for Paleoclimatology (https://www.ncdc.noaa.gov/paleo-search/?dataTypeId=18). The observed land surface temperature is available at the University of East Anglia-CRU's website (https://crudata.uea.ac.uk/cru/data/temperature/).

**Acknowledgments**
U. K. Thapa received research support from the NOAA Climate and Global Change Postdoctoral Fellowship Program, administered by UCAR's Cooperative Programs for the Advancement of Earth System Science under award NA18N-WS4620043B. S. Stevenson and M. Midhun were supported by NSF P2C2 award AGS-1805143. The CESM project is supported primarily by NSF. This material is based upon work supported by the National Center for Atmospheric Research, a major facility sponsored by the NSF under Cooperative Agreement No. 1852977.

## References

Ahmed, F., Adnan, S., & Latif, M. (2020). Impact of jet stream and associated mechanisms on winter precipitation in Pakistan. *Meteorology and Atmospheric Physics*, *132*(2), 225–238. https://doi.org/10.1007/s00703-019-00683-8

Archer, C. L., & Caldeira, K. (2008). Historical trends in the jet streams. *Geophysical Research Letters*, *35*(8), 1–6. https://doi.org/10.1029/2008GL033614

Barnes, E. A., & Polvani, L. (2013). Response of the midlatitude jets, and of their variability, to increased greenhouse gases in the CMIP5 models. *Journal of Climate*, *26*(18), 7117–7135. https://doi.org/10.1175/JCLI-D-12-00536.1

Barton, N. P., & Ellis, A. W. (2009). Variability in wintertime position and strength of the North Pacific jet stream as represented by re-analysis data. *International Journal of Climatology*, *29*, 851–862. https://doi.org/10.1002/joc.1750

Bell, B., Hersbach, H., Berrisford, P., Dahlgren, P., Horányi, A., Muñoz Sabater, J., et al. (2020). ERA5 monthly averaged data on pressure levels from 1950 to 1978 (preliminary version). Copernicus Climate Change Service (C3S) Climate Data Store (CDS). Retrieved from https://cds.climate.copernicus.eu/cdsapp#!/dataset/reanalysis-era5-pressure-levels-monthly-means-preliminary-back-extension?tab=overview

Belmecheri, S., Babst, F., Hudson, A. R., Betancourt, J., & Trouet, V. (2017). Northern Hemisphere jet stream position indices as diagnostic tools for climate and ecosystem dynamics. *Earth Interactions*, *21*(8), 1–23. https://doi.org/10.1175/EI-D-16-0023.1

Berger, A., & Loutre, M. F. (1991). Insolation values for the climate of the last 10 million years. *Quaternary Science Reviews*, *10*(4), 297–317. https://doi.org/10.1016/0277-3791(91)90033-Q

Biemans, H., Siderius, C., Lutz, A. F., Nepal, S., Ahmad, B., Hassan, T., et al. (2019). Importance of snow and glacier meltwater for agriculture on the Indo-Gangetic Plain. *Nature Sustainability*, *2*(7), 594–601. https://doi.org/10.1038/s41893-019-0305-3

Borisenkov, Y. P., Tsvetkov, A. V., & Agaponov, S. V. (1983). On some characteristics of insolation changes in the past and the future. *Climate Change*, *5*, 237–244. https://doi.org/10.1007/bf02423520

Cannon, F., Carvalho, L. M. V., Jones, C., & Bookhagen, B. (2015). Multi-annual variations in winter westerly disturbance activity affecting the Himalaya. *Climate Dynamics*, *44*(1–2), 441–455. https://doi.org/10.1007/s00382-014-2248-8

Cannon, F., Carvalho, L. M. V., Jones, C., & Norris, J. (2016). Winter westerly disturbance dynamics and precipitation in the western himalaya and karakoram: A wave-tracking approach. *Theoretical and Applied Climatology*, *125*(1–2), 27–44. https://doi.org/10.1007/s00704-015-1489-8

Capotondi, A., Deser, C., Phillips, A. S., Okumura, Y., & Larson, S. M. (2020). ENSO and pacific decadal variability in the community earth system model version 2. *Journal of Advances in Modeling Earth Systems*, *12*, e2019MS002022. https://doi.org/10.1029/2019MS002022

Coumou, D., Lehmann, J., & Beckmann, J. (2015). The weakening summer circulation in the Northern Hemisphere mid-latitudes. *Science*, *348*(6232), 324–327. https://doi.org/10.1126/science.1261768

Crowley, T. J. (2000). Causes of climate change over the past 1000 years. *Science*, *289*(5477), 270–277. https://doi.org/10.1126/science.289.5477.270

Davis, B. A. S., & Brewer, S. (2009). Orbital forcing and role of the latitudinal insolation/temperature gradient. *Climate Dynamics*, *32*(2–3), 143–165. https://doi.org/10.1007/s00382-008-0480-9

Dimri, A. P., Niyogi, D., Barros, A. P., Ridley, J., Mohanty, U. C., Yasunari, T., & Sikka, D. R. (2015). Western disturbances: A review. *Reviews of Geophysics*, *53*, 225–246. https://doi.org/10.1002/2014RG000460

Francis, J. A., & Vavrus, S. J. (2012). Evidence linking Arctic amplification to extreme weather in mid-latitudes. *Geophysical Research Letters*, *39*, L06801. https://doi.org/10.1029/2012GL051000

Fu, Q., Johanson, C. M., Wallace, J. M., & Reichler, T. (2006). Enhanced mid-latitude tropospheric warming in satellite measurements. *Science*, *312*(5777), 1179. https://doi.org/10.1126/science.1125566

Fu, Q., & Lin, P. (2011). Poleward shift of subtropical jets inferred from satellite-observed lower-stratospheric temperatures. *Journal of Climate*, *24*(21), 5597–5603. https://doi.org/10.1175/JCLI-D-11-00027.1

Grise, K. M., Davis, S. M., Staten, P. W., & Adam, O. (2018). Regional and seasonal characteristics of the recent expansion of the tropics. *Journal of Climate*, *31*(17), 6839–6856. https://doi.org/10.1175/JCLI-D-18-0060.1

Hersbach, H., Bell, B., Berrisford, P., Horányi, A., Muñoz Sabater, J., Nicolas, J., et al. (2018). ERA5 hourly data on pressure levels from 1979 to present. Copernicus climate change service (C3S) climate data store (CDS). https://doi.org/10.24381/cds.bd0915c6

Hu, Y., & Fu, Q. (2007). Observed poleward expansion of the Hadley circulation since 1979. *Atmospheric Chemistry and Physics*, *7*(19), 5229–5236. https://doi.org/10.5194/acp-7-5229-2007

Hunt, K. M. R., Curio, J., Turner, A. G., & Schiemann, R. (2018). Subtropical westerly jet influence on occurrence of western disturbances and Tibetan Plateau vortices. *Geophysical Research Letters*, *45*(16), 8629–8636. https://doi.org/10.1029/2018GL077734

Hunt, K. M. R., Turner, A. G., & Shaffrey, L. C. (2018). The evolution, seasonality and impacts of western disturbances. *Quarterly Journal of the Royal Meteorological Society*, *144*(710), 278–290. https://doi.org/10.1002/qj.3200

Immerzeel, W. W., Lutz, A. F., Andrade, M., Bahl, A., Biemans, H., Bolch, T., et al. (2020). Importance and vulnerability of the world's water towers. *Nature*, *577*(7790), 364–369. https://doi.org/10.1038/s41586-019-1822-y

Jiang, N., Yan, Q., & Wang, H. (2020). Variation of the summer Asian westerly jet over the last millennium based on the PMIP3 simulations. *The Holocene*, *30*(2), 332–343. https://doi.org/10.1177/0959683619883011

Kalnay, E., Kanamitsu, M., Kistler, R., Collins, W., Deaven, D., & Gandin, L. (1996). The NCEP/NCAR 40-year reanalysis project. *Bulletin of the American Meteorological Society*, *77*(3), 437–472. https://doi.org/10.1175/1520-0477(1996)077<0437:TNYRP>2.0.CO;2

Kobayashi, S., Ota, Y., Harada, Y., Ebita, A., Moriya, M., Onoda, H., et al. (2015). The JRA-55 reanalysis: General specifications and basic characteristics. *Journal of the Meteorological Society of Japan*, *93*(1), 5–48. https://doi.org/10.2151/jmsj.2015-001

Koch, P., Wernli, H., & Davies, H. C. (2006). An event-based jet-stream climatology and typology. *International Journal of Climatology*, *26*(3), 283–301. https://doi.org/10.1002/joc.1255

Koteswaram, P. (1953). An analysis of the high tropospheric wind circulation over India in winter. *Indian Journal of Meteorology and Geophysics*, *4*, 13–21.

Koteswaram, P., Raman, C., & Parthasarathy, S. (1953). The mean jet stream over India and Burma in winter. *Indian Journal of Meteorology and Geophysics*, *4*, 111–122.

Krishnan, R., & Ramanathan, V. (2002). Evidence of surface cooling from absorbing aerosols. *Geophysical Research Letters*, *29*(9), 54-1–54-4. https://doi.org/10.1029/2002gl014687

Kuang, X., & Zhang, Y. (2005). Seasonal variation of the east Asian subtropical westerly jet and its association with the heating field over east Asia. *Advances in Atmospheric Sciences*, *22*(6), 831–840. https://doi.org/10.1007/bf02918683

Laskar, J., Joutel, F., & Boudin, F. (1993). Orbital, precessional, and insolation quantities for the Earth from –20Myr to +10 Myr. *Astronomy and Astrophysics*, *270*, 522–533.

Lücke, L. J., Schurer, A. P., Wilson, R., & Hegerl, G. C. (2021). Orbital forcing strongly influences seasonal temperature trends during the last millennium. *Geophysical Research Letters*, *48*, e2020GL088776. https://doi.org/10.1029/2020GL088776

Madhura, R. K., Krishnan, R., Revadekar, J. V., Mujumdar, M., & Goswami, B. N. (2015). Changes in western disturbances over the western Himalayas in a warming environment. *Climate Dynamics*, *44*(3–4), 1157–1168. https://doi.org/10.1007/s00382-014-2166-9

Maher, P., Kelleher, M. E., Sansom, P. G., & Methven, J. (2020). Is the subtropical jet shifting poleward? *Climate Dynamics*, *54*(3–4), 1741–1759. https://doi.org/10.1007/s00382-019-05084-6

Mann, M. E., Rahmstorf, S., Kornhuber, K., Steinman, B. A., Miller, S. K., & Coumou, D. (2017). Influence of anthropogenic climate change on planetary wave resonance and extreme weather events. *Scientific Reports*, *7*, 45242. https://doi.org/10.1038/srep45242

Manney, G. L., & Hegglin, M. I. (2018). Seasonal and regional variations of long-term changes in upper-tropospheric jets from reanalyses. *Journal of Climate*, *31*(1), 423–448. https://doi.org/10.1175/JCLI-D-17-0303.1

Marcello, F., Wainer, I., Gent, P. R., Otto-Bliesner, B. L., & Brady, E. C. (2019). South Atlantic surface boundary current system during the last millennium in the CESM-LME: The medieval climate anomaly and little ice age. *Geosciences*, *9*(7), 1–18. https://doi.org/10.3390/geosciences9070299

Nie, Y., Pritchard, H. D., Liu, Q., Hennig, T., Wang, W., Wang, X., et al. (2021). Glacial change and hydrological implications in the Himalaya and Karakoram. *Nature Reviews Earth & Environment*, *2*(2), 91–106. https://doi.org/10.1038/s43017-020-00124-w

Otto-Bliesner, B. L., Brady, E. C., Fasullo, J., Jahn, A., Landrum, L., Stevenson, S., et al. (2016). Climate variability and change since 850 ce an ensemble approach with the community earth system model. *Bulletin of the American Meteorological Society*, *97*(5), 787–754. https://doi.org/10.1175/BAMS-D-14-00233.1

Pena-Ortiz, C., Gallego, D., Ribera, P., Ordonez, P., & Del Carmen Alvarez-Castro, M. (2013). Observed trends in the global jet stream characteristics during the second half of the 20th century. *Journal of Geophysical Research: Atmospheres*, *118*(7), 2702–2713. https://doi.org/10.1002/jgrd.50305

Ren, X., Yang, X., Zhou, T., & Fang, J. (2011). Diagnostic comparison of wintertime East Asian subtropical jet and polar-front jet: Large-scale characteristics and transient eddy activities. *Acta Meteorologica Sinica*, *25*(1), 21–33. https://doi.org/10.1007/s13351-011-0002-2

Rotstayn, L. D., Collier, M. A., Jeffrey, S. J., Kidston, J., Syktus, J. I., & Wong, K. K. (2013). Anthropogenic effects on the subtropical jet in the Southern Hemisphere: Aerosols versus long-lived greenhouse gases. *Environmental Research Letters*, *8*(1), 014030. https://doi.org/10.1088/1748-9326/8/1/014030

Schiemann, R., Lüthi, D., & Schär, C. (2009). Seasonality and interannual variability of the westerley jet in the Tibetan Plateau region. *Journal of Climate*, *22*(11), 2940–2957. https://doi.org/10.1175/2008JCLI2625.1

Seidel, D. J., Fu, Q., Randel, W. J., & Reiohler, T. J. (2008). Widening of the tropical belt in a changing climate. *Nature Methods*, *1*(1), 21–24. https://doi.org/10.1038/ngeo.2007.38

Servonnat, J., Yiou, P., Khodri, M., Swingedouw, D., & Denvil, S. (2010). Influence of solar variability, $CO_2$ and orbital forcing between 1000 and 1850 AD in the IPSLCM4 model. *Climate of the Past*, *6*(4), 445–460. https://doi.org/10.5194/cp-6-445-2010

Slivinski, L. C., Compo, G. P., Whitaker, J. S., Sardeshmukh, P. D., Giese, B. S., McColl, C., et al. (2019). Towards a more reliable historical reanalysis: Improvements for version 3 of the Twentieth Century Reanalysis system. *Quarterly Journal of the Royal Meteorological Society*, *145*(724), 2876–2908. https://doi.org/10.1002/qj.3598

Staten, P. W., Lu, J., Grise, K. M., Davis, S. M., & Birner, T. (2018). Re-examining tropical expansion. *Nature Climate Change*, *8*(9), 768–775. https://doi.org/10.1038/s41558-018-0246-2

Stevenson, S., Capotondi, A., Fasullo, J., & Otto-Bliesner, B. (2017). Forced changes to twentieth century ENSO diversity in a last millennium context. *Climate Dynamics*, *52*(12), 7359–7374. https://doi.org/10.1007/s00382-017-3573-5

Stevenson, S., Fasullo, J. T., Otto-Bliesner, B. L., Tomas, R. A., & Gao, C. (2017). Role of eruption season in reconciling model and proxy responses to tropical volcanism. *Proceedings of the National Academy of Sciences of the United States of America*, *114*(8), 1822–1826. https://doi.org/10.1073/pnas.1612505114

Stevenson, S., Overpeck, J. T., Fasullo, J., Coats, S., Parsons, L., Otto-Bliesner, B., et al. (2018). Climate variability, volcanic forcing, and last millennium hydroclimate extremes. *Journal of Climate*, *31*(11), 4309–4327. https://doi.org/10.1175/JCLI-D-17-0407.1

Strong, C., & Davis, R. E. (2007). Winter jet stream trends over the Northern Hemisphere. *Quarterly Journal of the Royal Meteorological Society*, *133*, 2109–2115. https://doi.org/10.1002/qj.171

Thapa, U. K., St George, S., & Trouet, V. (2020). Poleward excursions by the Himalayan subtropical jet over the past four centuries. *Geophysical Research Letters*, *47*(22), 1–10. https://doi.org/10.1029/2020GL089631

Touma, D., Stevenson, S., Lehner, F., & Coats, S. (2021). Human-driven greenhouse gas and aerosol emissions cause distinct regional impacts on extreme fire weather. *Nature Communications*, *12*(1), 1–8. https://doi.org/10.1038/s41467-020-20570-w

Trouet, V., Babst, F., & Meko, M. (2018). Recent enhanced high-summer North Atlantic Jet variability emerges from three-century context. *Nature Communications*, *9*(1), 1–9. https://doi.org/10.1038/s41467-017-02699-3

Wang, W., Zhou, W., Wang, X., Fong, S. K., & Leong, K. C. (2013). Summer high temperature extremes in Southeast China associated with the East Asian jet stream and circumglobal teleconnection. *Journal of Geophysical Research: Atmospheres*, *118*(15), 8306–8319. https://doi.org/10.1002/jgrd.50633

Wilcox, L. J., Hoskins, B. J., & Shine, K. P. (2012). A global blended tropopause based on ERA data. Part II: Trends and tropical broadening. *Quarterly Journal of the Royal Meteorological Society*, *138*(664), 576–584. https://doi.org/10.1002/qj.910

Wright, W. E., Guan, B. T., Tseng, Y. H., Cook, E. R., Wei, K. Y., & Chang, S. T. (2015). Reconstruction of the springtime East Asian subtropical jet and Western Pacific pattern from a Millennial-Length Taiwanese Tree-Ring chronology. *Climate Dynamics*, *44*(5–6), 1645–1659. https://doi.org/10.1007/s00382-014-2402-3

Yin, J. H. (2005). A consistent poleward shift of the storm tracks in simulations of 21st century climate. *Geophysical Research Letters*, *32*(18), 1. https://doi.org/10.1029/2005GL023684

Zhang, Y., Kuang, X., Guo, W., & Zhou, T. (2006). Seasonal evolution of the upper-tropospheric westerly jet core over East Asia. *Geophysical Research Letters*, *33*(11), 3–6. https://doi.org/10.1029/2006GL026377

Zhongda, L., & Riyu, L. U. (2005). Interannual meridional displacement of the East Asian upper-tropospheric jet stream in summer. *Advances in Atmospheric Sciences*, *22*(2), 199–211. https://doi.org/10.1007/bf02918509

Zhou, W., Xie, S.-P., & Yang, D. (2019). Enhanced equatorial warming causes deep-tropical contraction and subtropical monsoon shift. *Nature Climate Change*, *9*(11), 834–839. https://doi.org/10.1038/s41558-019-0603-9

## References From the Supporting Information

Cook, E. R., Krusic, P. J., Anchukaitis, K. J., Buckley, B. M., Nakatsuka, T., & Sano, M. (2013). Tree-ring reconstructed summer temperature anomalies for temperate East Asia since 800 C.E. *Climate Dynamics*, *41*(11–12), 2957–2972. https://doi.org/10.1007/s00382-012-1611-x

Huang, B., Thorne, P. W., Banzon, V. F., Boyer, T., Chepurin, G., Lawrimore, J. H., et al. (2017). Extended reconstructed Sea surface temperature, Version 5 (ERSSTv5): Upgrades, validations, and intercomparisons. *Journal of Climate*, *30*(20), 8179–8205. https://doi.org/10.1175/JCLI-D-16-0836.1

Morice, C. P., Kennedy, J., Rayner, N. A., Winn, J. P., Hogan, E., Killick, R. E., et al. (2021). An updated assessment of near-surface temperature change from 1850 : The HadCRUT5 data set. *Journal of Geophysical Research: Atmospheres*, *126*, e2019JD032361. https://doi.org/10.1029/2019JD032361